

Conrad Deep: a new northern Red Sea deep. Origin and implications for continental rifting

James R. Cochran, Fernando Martinez, Michael S. Steckler and Michael A. Hobart

Lamont-Doherty Geological Observatory of Columbia University, Palisades, NY 10964 (U.S.A.)

Received October 21, 1985; revised version received February 3, 1986

A previously unknown deep, here called Conrad Deep, was discovered during an extensive geophysical survey of the northern Red Sea in June, 1984. Conrad Deep is located at 27°03'N, 34°43'E, only 90 km south of the Gulf of Suez and is the most northern deep yet discovered in the Red Sea. It is located within a well developed axial depression which also contains Charcot Deep, 100 km to the south. The axial depression is associated with abundant recent deformation and is situated at the peak of a regional heat flow high extending across the rift. Conrad Deep is typical of the small northern type Red Sea Deep. It is 10 km long, 2 km wide and has a maximum depth of 1460 m. It is associated with high and variable heat flow values and large magnetic anomalies. There is no evidence of a dense brine layer. Detailed analysis of the geophysical data implies that the deep probably results from a very recent (< 40,000 years) intrusion into continental type basement. The formation of a well defined axial depression associated with very high heat flow and small deeps resulting from isolated intrusions may be the first step in the transition from continental extension to seafloor spreading.

1. Introduction

The Red Sea can be divided into three distinct and different sections, each characterized by different morphology and structure (Fig. 1). Each of these sections appears to represent a different stage in the development of a continental margin and establishment of a mid-ocean ridge spreading system [1].

The southern Red Sea, between 15°N and 20°N, is characterized by a well developed axial trough which has developed through normal seafloor spreading during the last five million years [2]. The axial trough becomes discontinuous north of 20°N and a transition zone is located from there to about 23°20'N in which the central Red Sea consists of a series of “deeps” alternating with shallower “intertrough zones” [3]. The northern Red Sea consists of a broad trough without a recognizable spreading center, although there are a number of small, isolated deeps.

The purpose of this paper is to discuss some of the results of a 1984 cruise of the R.V. “Robert D. Conrad” in the northern Red Sea. We will describe a small, well-defined, elongated deep which we call the “Conrad Deep” and discuss the origin

of the small northern Red Sea deeps and their significance for the nature of the extension occurring between Africa and Arabia and for the transition from continental rifting to seafloor spreading.

2. Red Sea deeps

A characteristic feature of the Red Sea is the presence of a series of “deeps” which occupy the axial section of the central and northern Red Sea and are associated with hot brines and metalliferous sediments [4–6] (Fig. 1). The best known and most studied are a series of large well developed deeps between 20°N and 23°20'N. These deeps are similar in appearance to the axial trough spreading center found in the southern Red Sea, with steep sides, a rough bottom and large magnetic anomalies [3,4] (Fig. 2). Numerous heat flow measurements in the Atlantis II Deep and Nereus Deep show high heat flow with large local variability [7,8]. The heat flow pattern along with the presence of hot, metalliferous brines in a number of the deeps implies vigorous hydrothermal circulation and a shallow heat source. Basalt has been recovered from central volcanic ridges in several of the deeps [8] supporting the hypothesis that they

are discontinuous segments of a mid-ocean ridge type spreading center [1,9].

In contrast, the intertrough zones which separate the deeps are shallower with gently sloping sides, a smoother bottom and no significant magnetic anomalies (Fig. 2). The intertrough zones are underlain by at least 800 m (0.9 s) of sediments and Upper Miocene Reflector S (top of the

evaporites) is continuous across the axis of the Red Sea within them [3].

Seafloor spreading anomaly 2 (1.7 m.y. B.P.) is not present at the Atlantis II Deep or Nereus Deep [3] suggesting that seafloor spreading has only recently started in the deeps and that the intertrough zones represent regions in which an organized spreading center has not yet become established.

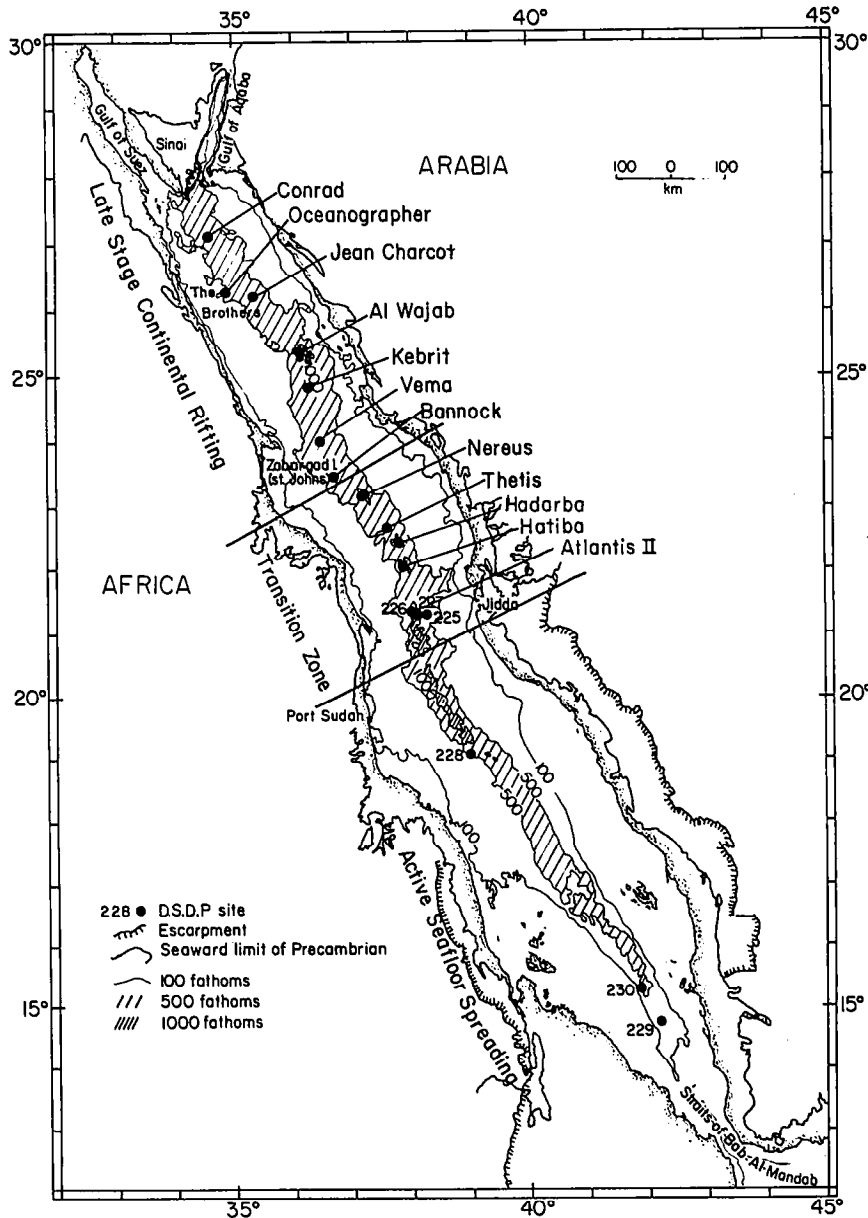


Fig. 1. Map of the Red Sea showing division into three sections representing different stages in the development of the margin. Location of "deeps" is also indicated.

Nereus Deep, which extends from about 23°N to 23°20'N, is the furthest north of the large well developed deeps (Fig. 2). North of Nereus Deep there are no morphologically or geophysically identifiable features in the northern Red Sea that can be interpreted as localized spreading centers. Early seismic reflection studies in the northern Red Sea [10,11] showed that Upper Miocene Reflector S is continuous across the axis, that the upper surface of the evaporites is deformed and that the deformation, although most severe in the center, extends completely across the sea.

There is a series of isolated deeps in the northern portion of the Red Sea, some of which are also characterized by hot brines and metalliferous sediments [5,6] and which are usually, although not always, associated with large amplitude magnetic anomalies. The difference between the large, well developed transition zone deeps and the smaller northern Red Sea deeps can be seen in Fig. 2. Bannock and Vema Deeps are both significantly shallower and smaller than Nereus Deep. They are 15 km long, less than 5 km wide and reach maximum depths of about 1600 m [8,12] and both have

relatively flat sediment covered bottoms. A small peak, from which dolerite has been dredged and which is associated with a large magnetic anomaly, is located in Bannock Deep [8]. No igneous rock has been recovered from Vema deep and a large magnetic anomaly is not observed there.

Until recently, the only other axial deeps reported in the northern Red Sea were Kebrit Deep at 24°44'N and Al Wajab Deep near 25°20'N. Oceanographer Deep at 26°17'N, an off-axis deep, is a small oval depression about 1 km across which is well away from the center of the Red Sea near the Brothers Islands [5,6] with which it may be tectonically related.

Recently Pautot et al. [13] reported the discovery of the Jean Charcot Deep at 26°15'N. Charcot Deep is 10 km long, 6 km wide with a maximum depth of 1490 m. It has a central ridge from which volcanic rocks have been recovered and is associated with a large magnetic anomaly.

3. Conrad Deep

During the summer of 1984, R.V. "Robert D. Conrad" conducted an extensive geophysical study

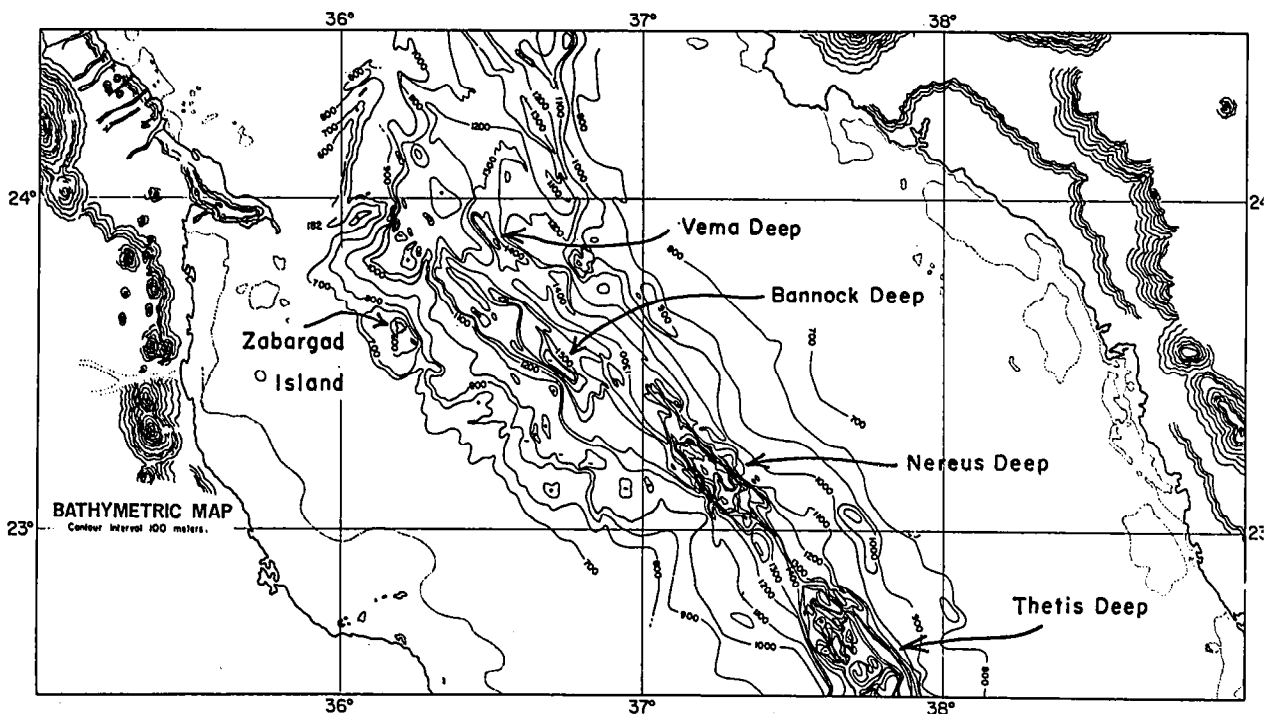


Fig. 2. Map of Central Red Sea spanning the boundary between the Transition Zone and the northern Red Sea region of continental rifting. Note difference in morphology between Thetis and Nereus Deeps, the northernmost of the transition zone deeps, and Bannock and Vema deeps, the southernmost of the northern Red Sea deeps. From Bonatti et al. [8].

of the area north of 26°N in the Red Sea. One result of this survey was the discovery of a previously unknown deep at $27^{\circ}03'\text{N}$, $34^{\circ}43'\text{E}$ which we will refer to as Conrad Deep. It is slightly more than 100 km north-northwest of Charcot Deep and 90 km south of Ras Muhammed, the southern tip of the Sinai Peninsula. Small deeps are thus found along the entire length of the northern Red Sea and appear to form an integral part of the tectonic processes occurring there.

The deep is located in the center of the Red Sea within a 20–30 km wide axial depression (Fig. 3)

which is a consistent feature of the Red Sea throughout the survey area. It is characterized by depths generally in the range of 1100–1250 m and is often, although not always, bounded by scarps of up to a few hundred meters height. However, unlike the axial trough of the southern Red Sea, this shallow depression is completely covered with a thick sedimentary layer including Upper Miocene Reflector S (Fig. 4). Charcot Deep, near the southern end of the survey area, is also located in the axial depression. The small, oval shaped Oceanographer Deep is located outside the axial depression

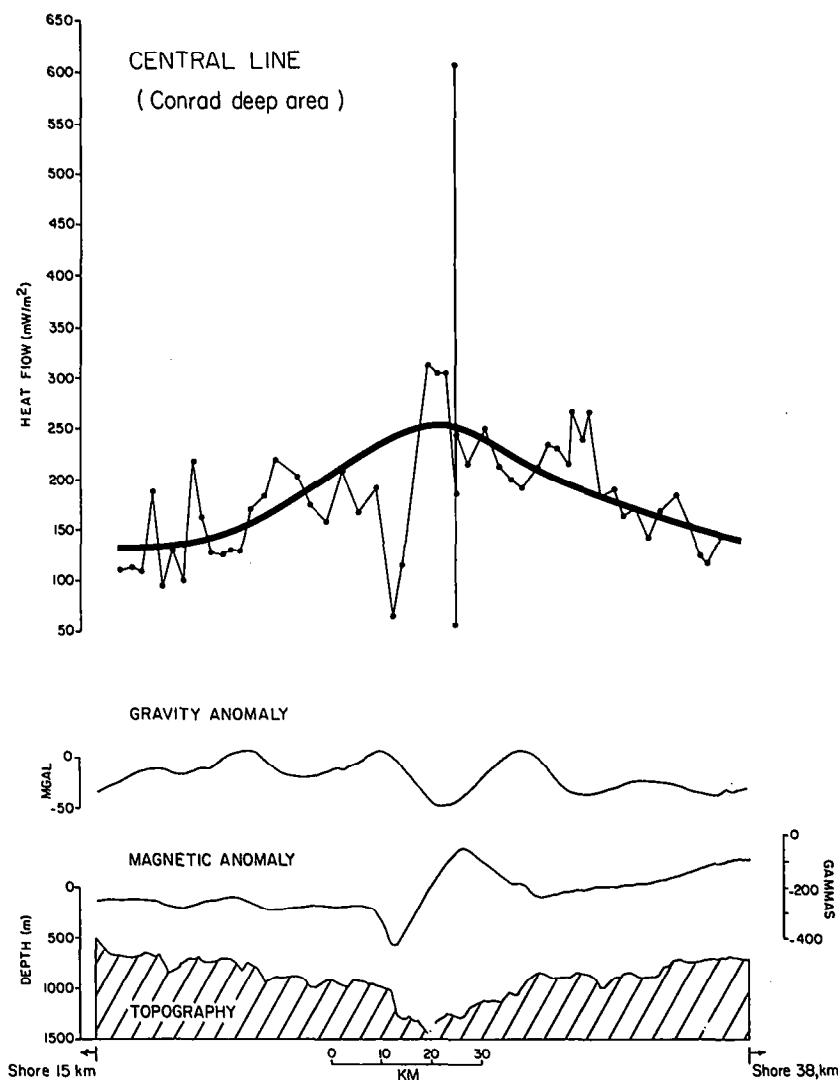


Fig. 3. Heat flow, free air gravity anomaly, total intensity magnetic anomaly and bathymetry profiles over Conrad Deep projected at $\text{N}60^{\circ}\text{E}$. Extremely high heat flow value of 605 mW m^{-2} occurs within the deep but appears displaced here because the trend of the deep is not perpendicular to the projection (see Fig. 4). The heavy line in the heat flow plot was fit by eye to indicate the overall trend in the data.

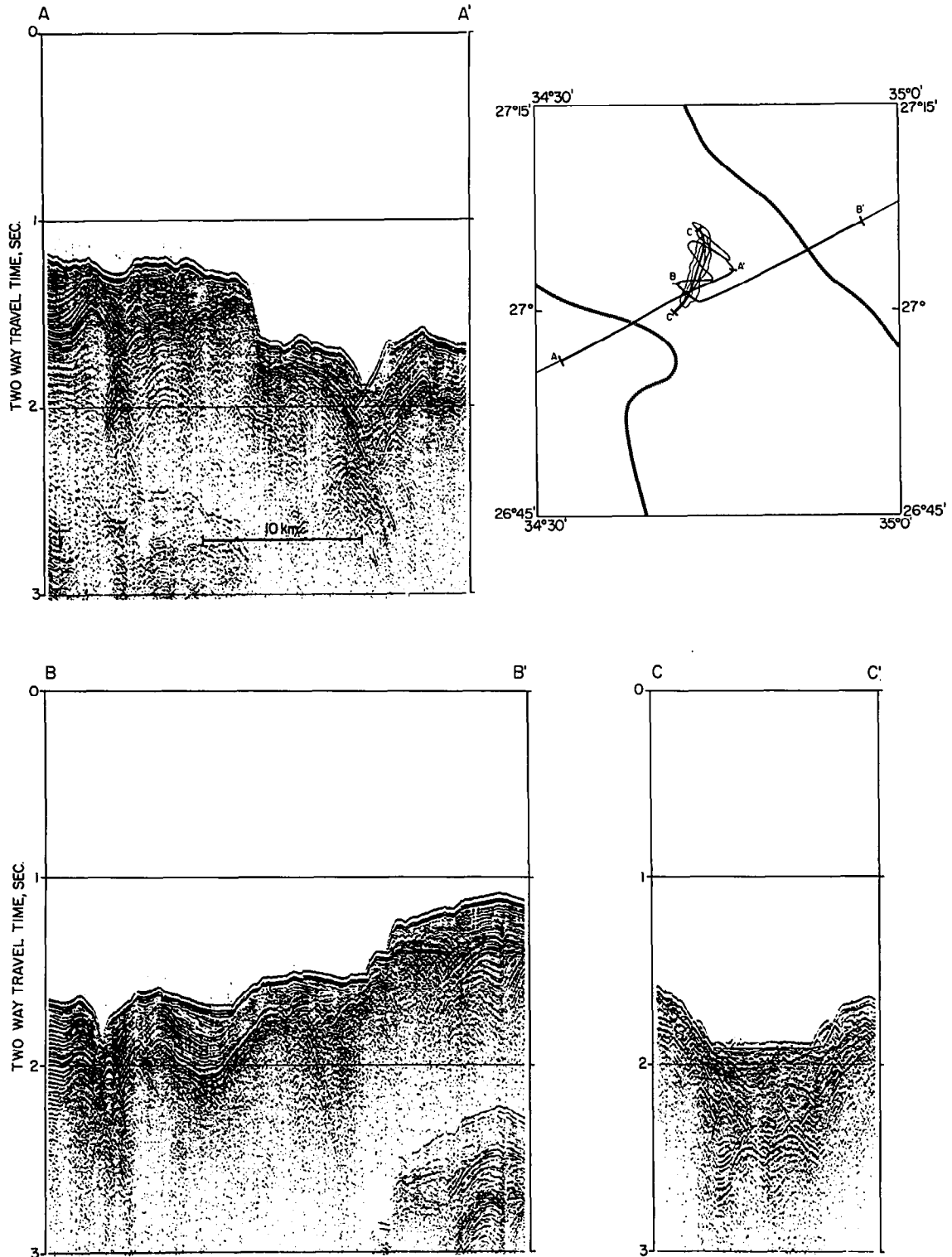


Fig. 4. Single channel water gun seismic reflection profiles across Conrad Deep. Lines AA' and BB' also cross the boundary between the marginal areas and the axial depression which is marked here by fault scarps. Reflector S is seen as strong arrivals that occur 0.2–0.4 seconds below the seafloor under both marginal regions and axial depression. Location map shows the position of the profiles in relation to the scarps bounding the axial depression (heavy dashed line) and Conrad Deep (outline). Approximate horizontal scale is indicated.

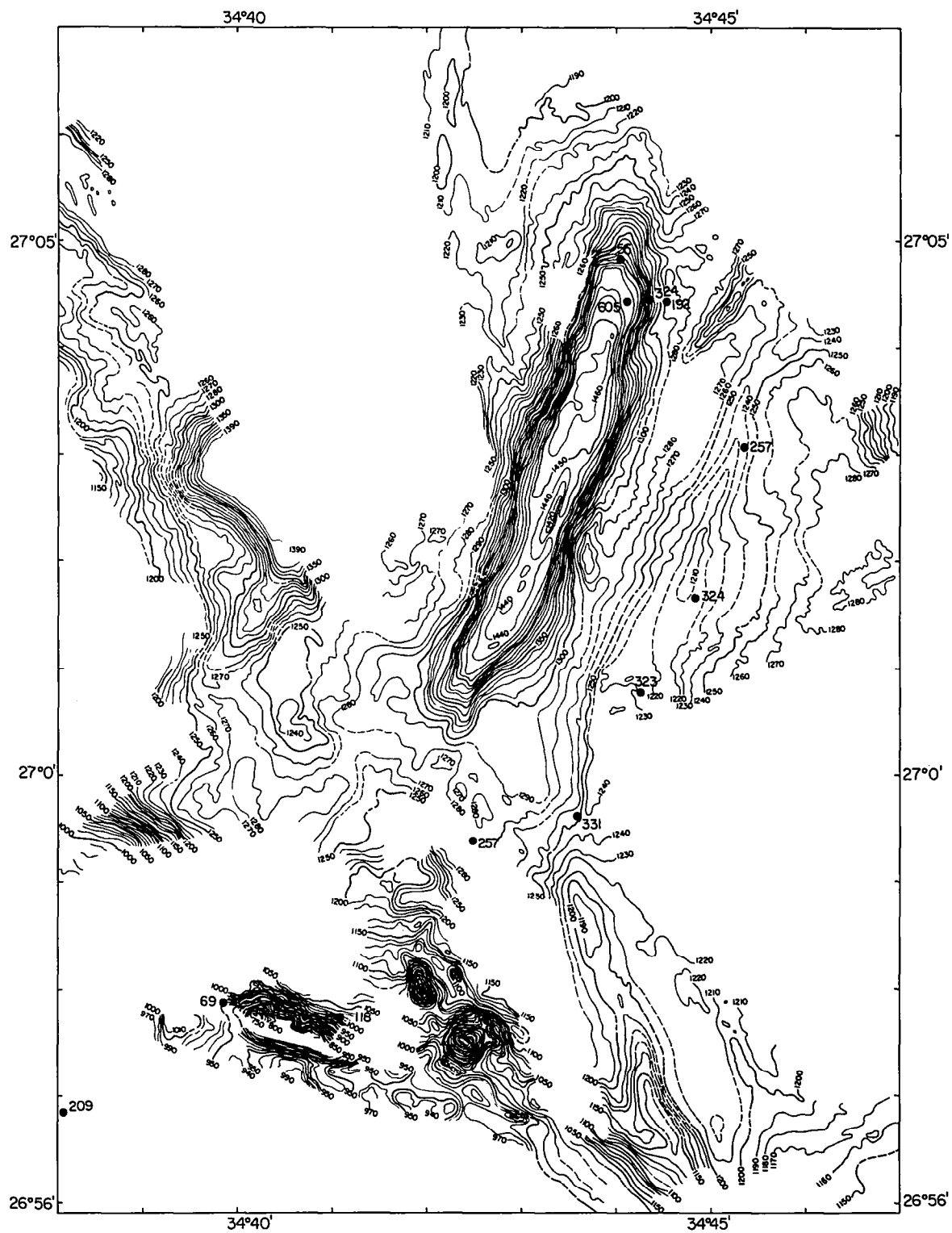


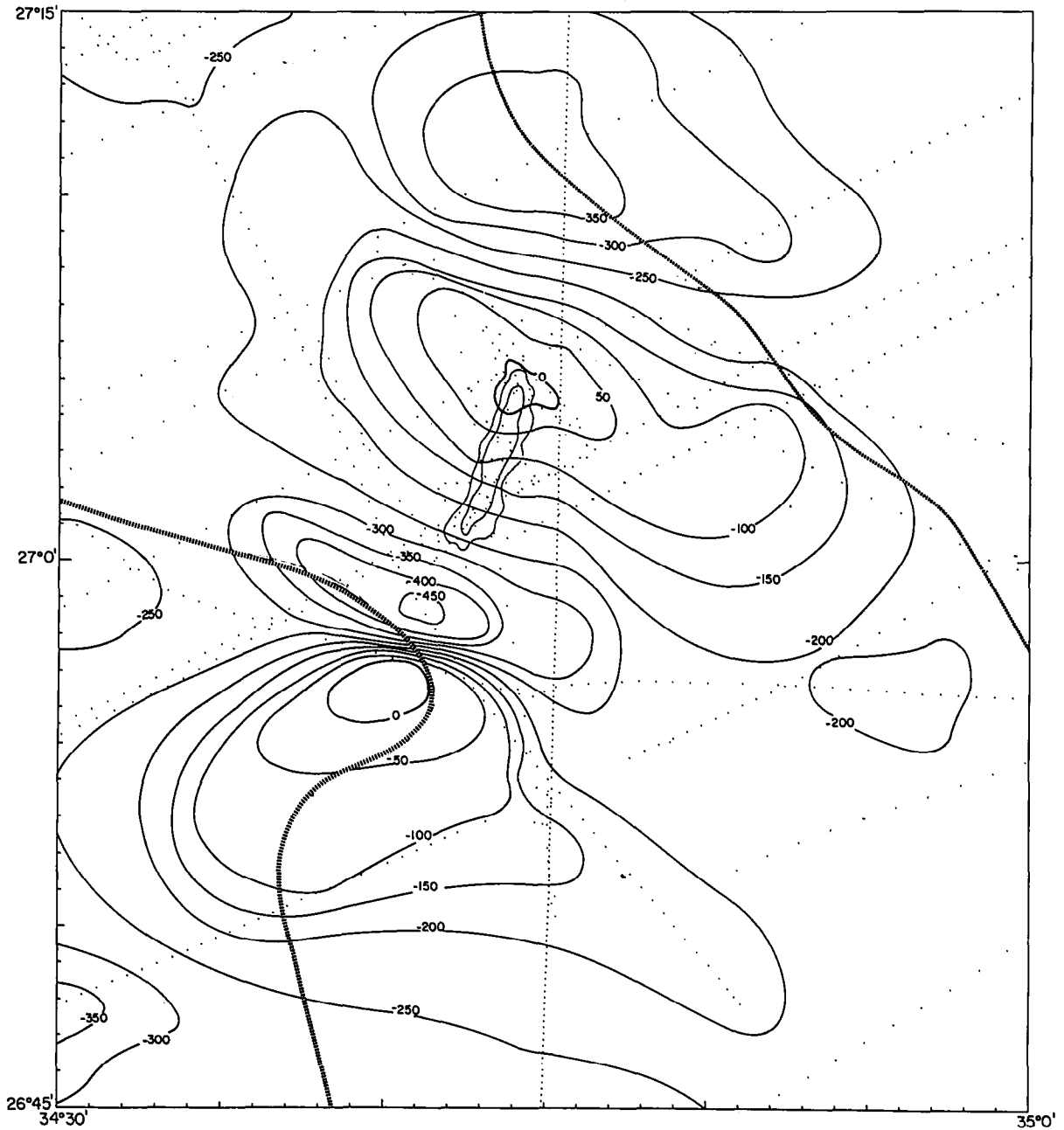
Fig. 5. Seabeam map of Conrad Deep. Contours are at 10 m intervals. Sound velocity of 1500 m s^{-1} assumed. Heat flow values in mW m^{-2} are indicated by bold numbers.

approximately 35 km west of Charcot Deep. About 25 km north of Conrad Deep, the position of the axial depression shifts from the center of the Red Sea toward the west so that it is aligned with the entrance to the Gulf of Suez.

Conrad Deep is a steep sided trough 10 km long and 1-2 km wide with the long axis oriented

N20°E, parallel to the trend of Gulf of Aqaba. A Seabeam survey of the deep (Fig. 5) showed it to have a relatively flat bottom sloping down from about 1440 m in the south to 1460 m in the north with a small ridge 30 m high, approximately 300 m wide and 1.6 km long occupying the central part of the deep. A small rise surrounds the deep at a

(A) CONRAD DEEP MAGNETIC ANOMALIES



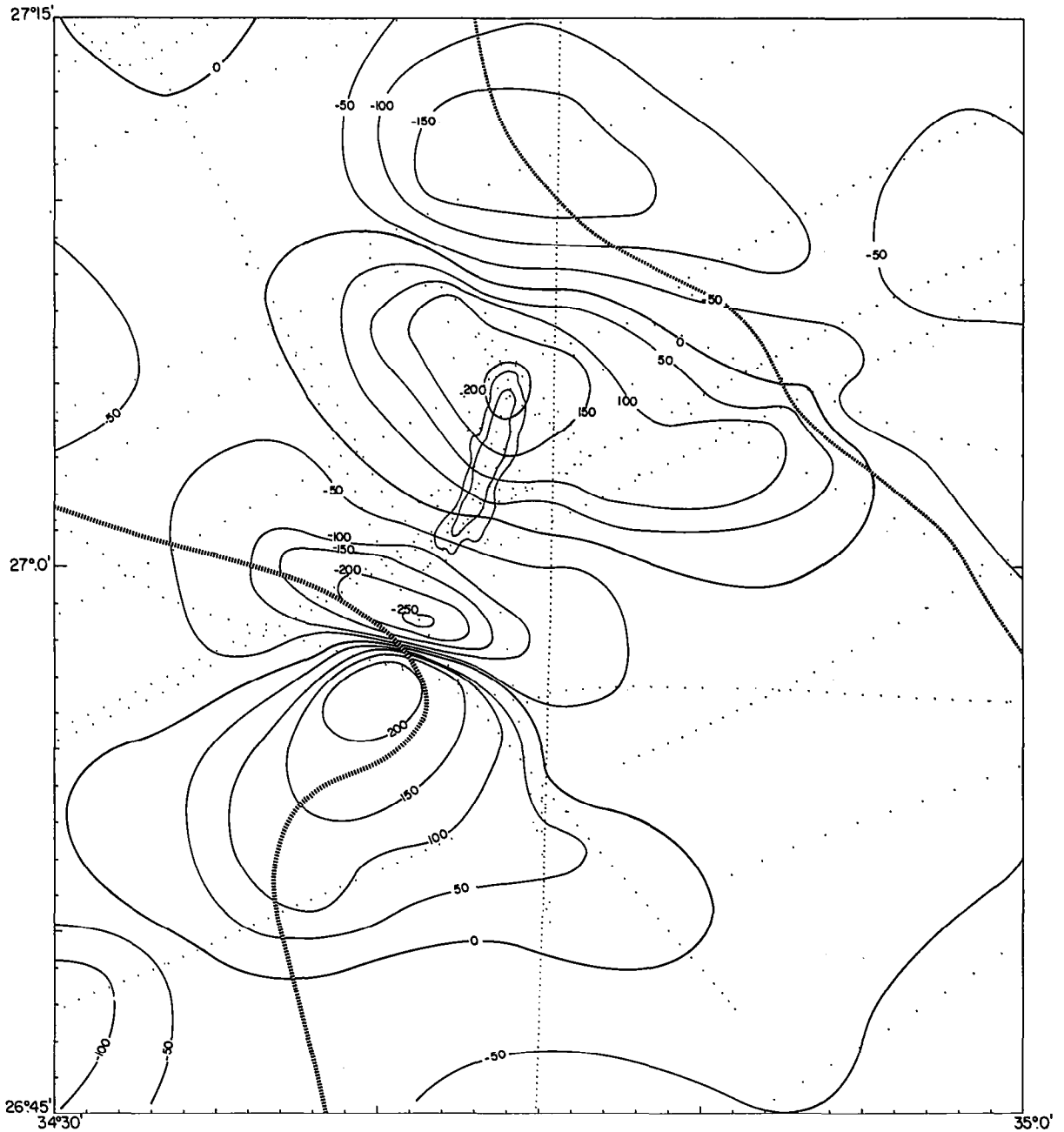
(B) CONRAD DEEP MAGNETIC ANOMALIES (regional field removed)

Fig. 6. A. Observed total field magnetic anomalies over Conrad Deep. Contour interval is 50 gammas. Control is indicated by small dots. Data is from 1984 Conrad and 1978 Jean Charcot cruises. Conrad Deep is outlined by fine lines near the center of the figure. Boundary of axial depression shown by heavy dashed lines. B. Total field magnetic anomalies over Conrad Deep with regional field removed by subtracting a best fitting plane from the data. Contour interval is 50 gammas.

distance of 2–4 km. Several oval-shaped features approximately 1 km in diameter and 150 m high are located in line with the southern end of Con-

rad Deep at the base of the scarp forming the boundary of the axial depression (Fig. 5). These may be small salt diapirs.

Seismic reflection data (Fig. 4) show that sub-bottom Reflector S, which has been shown to be the top of a massive Miocene evaporite sequence [14,16], is found at a depth of 0.2–0.3 s below the seafloor beneath the axial depression. Reflector S

can be identified to the edge of Conrad Deep, but becomes disturbed and difficult to follow beneath the deep on either transverse or longitudinal profiles (Fig. 4) although a strong reflector is found beneath the deep at a depth of 0.5–0.6 s below the

CONRAD DEEP FREE-AIR GRAVITY ANOMALIES

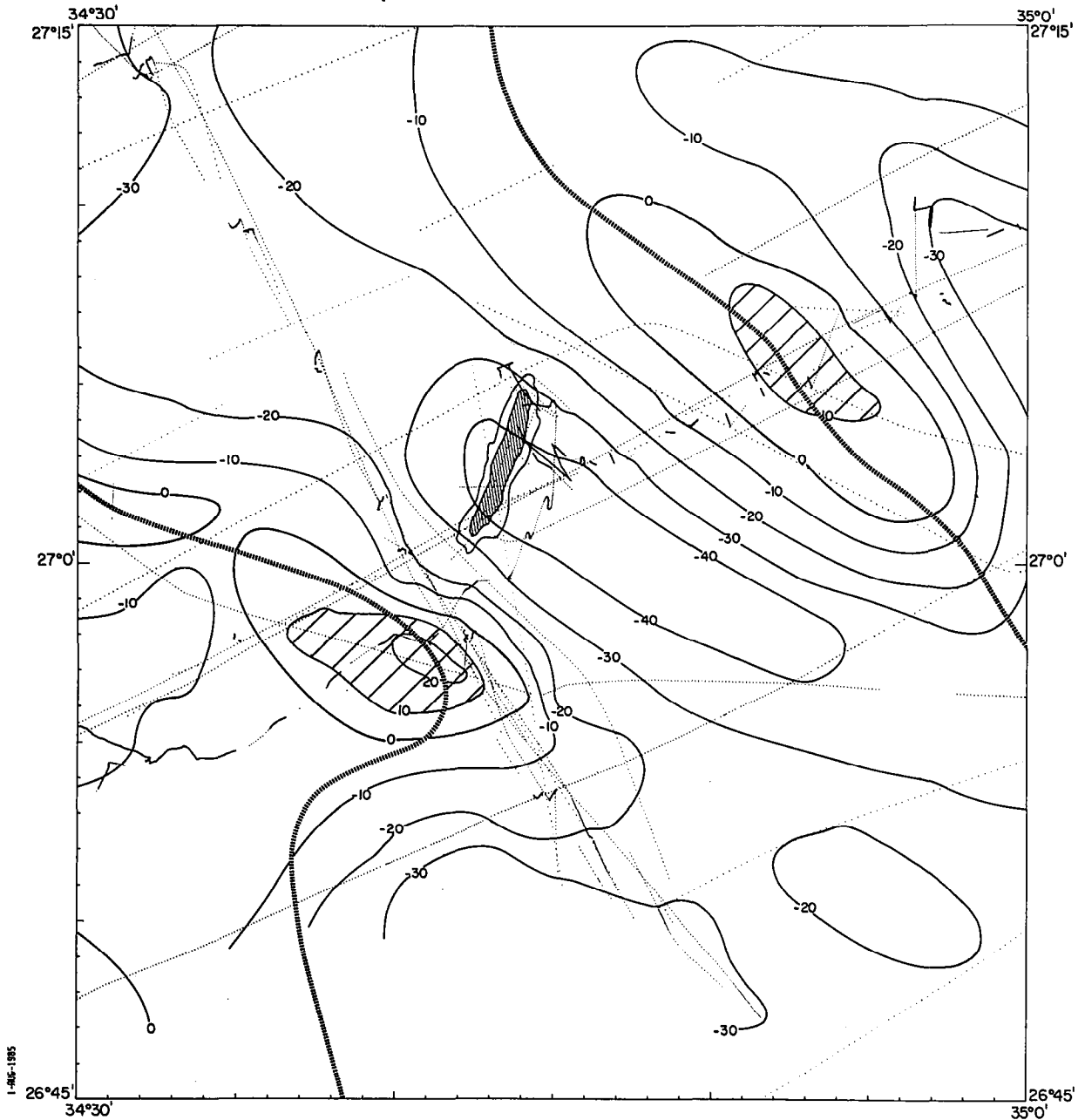


Fig. 7. Free air gravity anomalies in region of Conrad Deep contoured at 10 mgal intervals with control shown as fine dots. Conrad Deep is indicated with hachured outline. Boundaries of axial depression shown as heavy dashed lines. Areas with anomalies greater than +10 mgal are ruled.

seafloor. Since this reflector is present on both the lines crossing the deep and those running along it, the reflector is probably real and not a side echo or other artifact.

Conrad Deep is associated with large amplitude magnetic anomalies (Figs. 3, 6) which in map view take the form of two dipole pairs (Fig. 6A). The center of the northern dipole is located in line with the axis of the deep, but about 5 km to the north. The center of the southern dipole also occurs in line with the deep and lies 5 km to the south. Note that the maximum amplitude of the southern positive anomaly is not well constrained by our data.

Free-air gravity anomalies (Figs. 3, 7) show a strong NW-SE lineation reflecting the large-scale trends in the bathymetry. The axial depression is associated with a large-amplitude gravity low with a magnitude of about -40 mgals. Free-air gravity highs of magnitude $15-25$ mgals are found coincident with the scarps marking the boundary of the axial depression. No free-air gravity anomaly can be directly associated with the deep and the gravity trends cut almost perpendicularly across it.

The axial depression is associated with the center of a broad heat flow high extending completely across the Red Sea shown in Fig. 3. The details of the measurements comprising this heat flow profile will be presented elsewhere. The heat flow values in the vicinity of Conrad Deep are shown in Fig. 5. The mean of the values in the axial depression, excluding those in the Conrad Deep and two values at the base of the scarp to the southwest, is 285 ± 40 mW m^{-2} (6.8 ± 1.0 $\mu\text{cal cm}^{-2} \text{s}^{-1}$). Four measurements were made on the floor and the slopes of the northern end of Conrad Deep. The highest value was found on the floor, 605 mW m^{-2} ; the other values decreased steadily up the walls of the deep. An unusually low value of 56 mW m^{-2} , was measured on the northern wall of the deep. The bottom water temperature at the floor of the deep is 21.52°C , 0.04°C greater than temperatures in the surrounding waters outside the deep. No water column reflector was observed on the 3.5 kHz echo sounder during our survey of the deep and there is no evidence of a hot brine layer.

4. Discussion

The Red Sea deeps, both the large transition zone deeps and the smaller northern deeps, are

commonly attributed to intrusions, and volcanic rocks have been recovered from a number of them [8,13]. The relationship of the deeps to igneous activity is further demonstrated by the frequent coincidence of large amplitude magnetic anomalies with the deeps. The transition zone deeps between 20°N and 23°N (Fig. 1) are associated with lineated magnetic anomalies [3,8] and appear to be small seafloor spreading cells. Where there are magnetic anomalies over the smaller northern Red Sea deeps they are not lineated, but rather take the form of dipole pairs [8,13] suggesting that they result from isolated intrusions into a relatively non-magnetic crust.

The magnetic anomalies surrounding Conrad Deep take the form of a pair of dipoles and three-dimensional modeling shows that two sources are required to explain them (Fig. 8A, B). A single source extending under the deep would produce a magnetic high over its southern end and a magnetic low over its northern end rather than a pair of anomalies. The sources must be located under the region of steepest magnetic gradients and are thus about 5 km to the north and to the south of the deep in line with it near the edges of the axial depression. Although the location of the sources is well determined, the exact dimensions and depths are not well constrained as demonstrated by the source pairs in Fig. 8A and B, although bodies elongated perpendicular to the deep better reproduce the elongation of the observed anomalies.

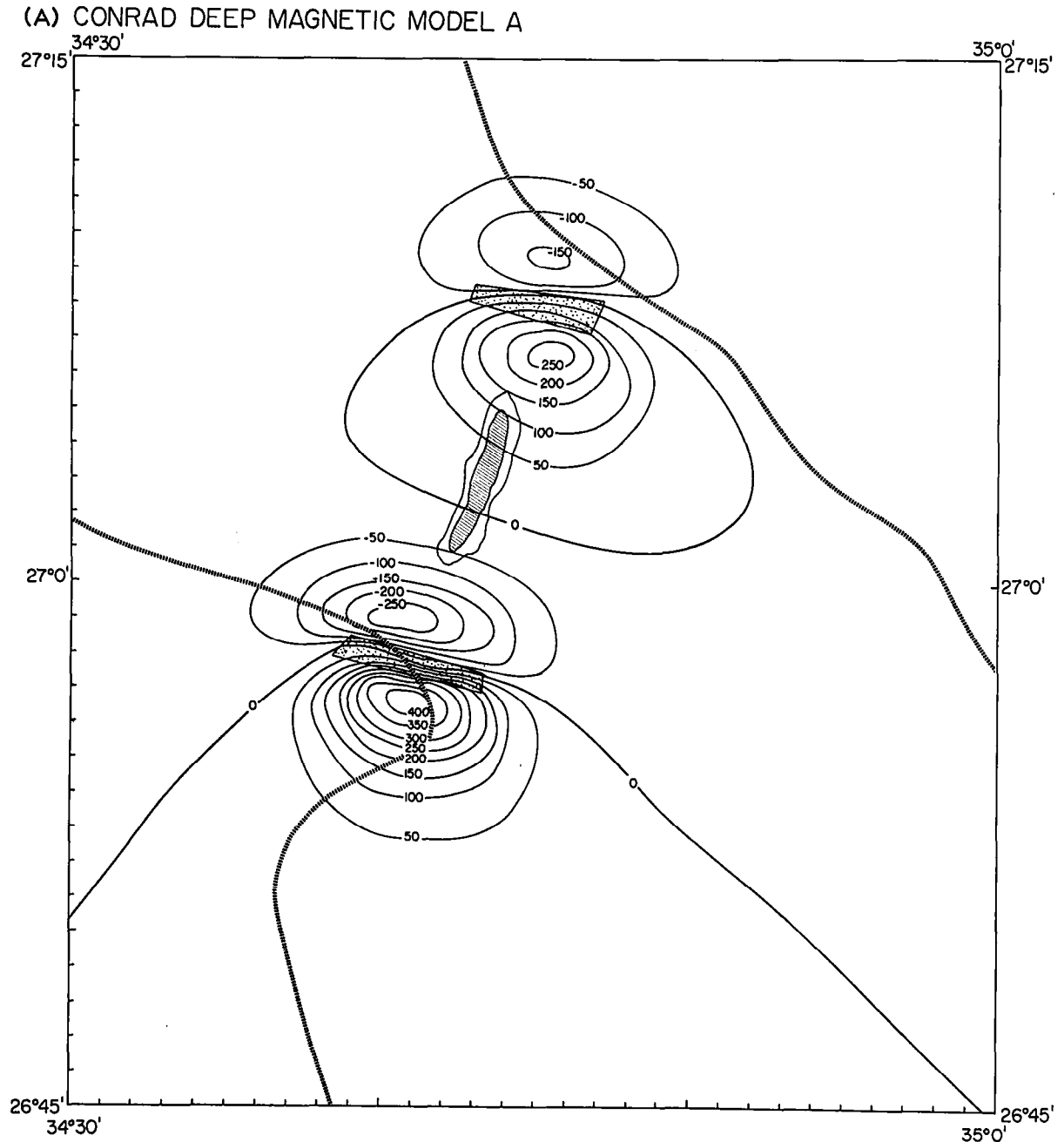
For a magnetization of 30 A m^{-1} , approximately 10 km^3 of magnetized material are required for each of the sources perpendicular to the deep (Fig. 8A). The sources parallel to the deep (Fig. 8B) are 12 km^3 and 35 km^3 in volume for the southern and northern sources respectively. The greater volume for the northern body results from the fact that it must be placed deeper to match the shape of the observed anomalies.

The axial depression is fault bounded in the vicinity of Conrad Deep and it is possible that igneous material was intruded along these faults to form two distinct bodies (Fig. 8A). A second explanation is that the deep results from the intrusion of a single dike which underlies the bathymetric deep and extends to the faults bounding the axial depression. This explanation accounts for the morphological expression of the deep and the high heat flow associated with it. The observed mag-

netic anomalies could then result from the fact that it was intruded so recently that only the tips of the dike have cooled sufficiently to acquire a remanent magnetization (Fig. 8B).

This possibility may be investigated by modeling the cooling of a rectangular dike in three dimensions. The method used is an adaptation of

a technique developed by Steckler [17]. We consider the dike to have been intruded at a constant temperature T_0 and to extend from a depth d below the seafloor to a depth where the regional temperature reaches T_0 . We will assume a linear temperature gradient consistent with the regional heat flow. The temperature distribution resulting



(B) CONRAD DEEP MAGNETIC MODEL B

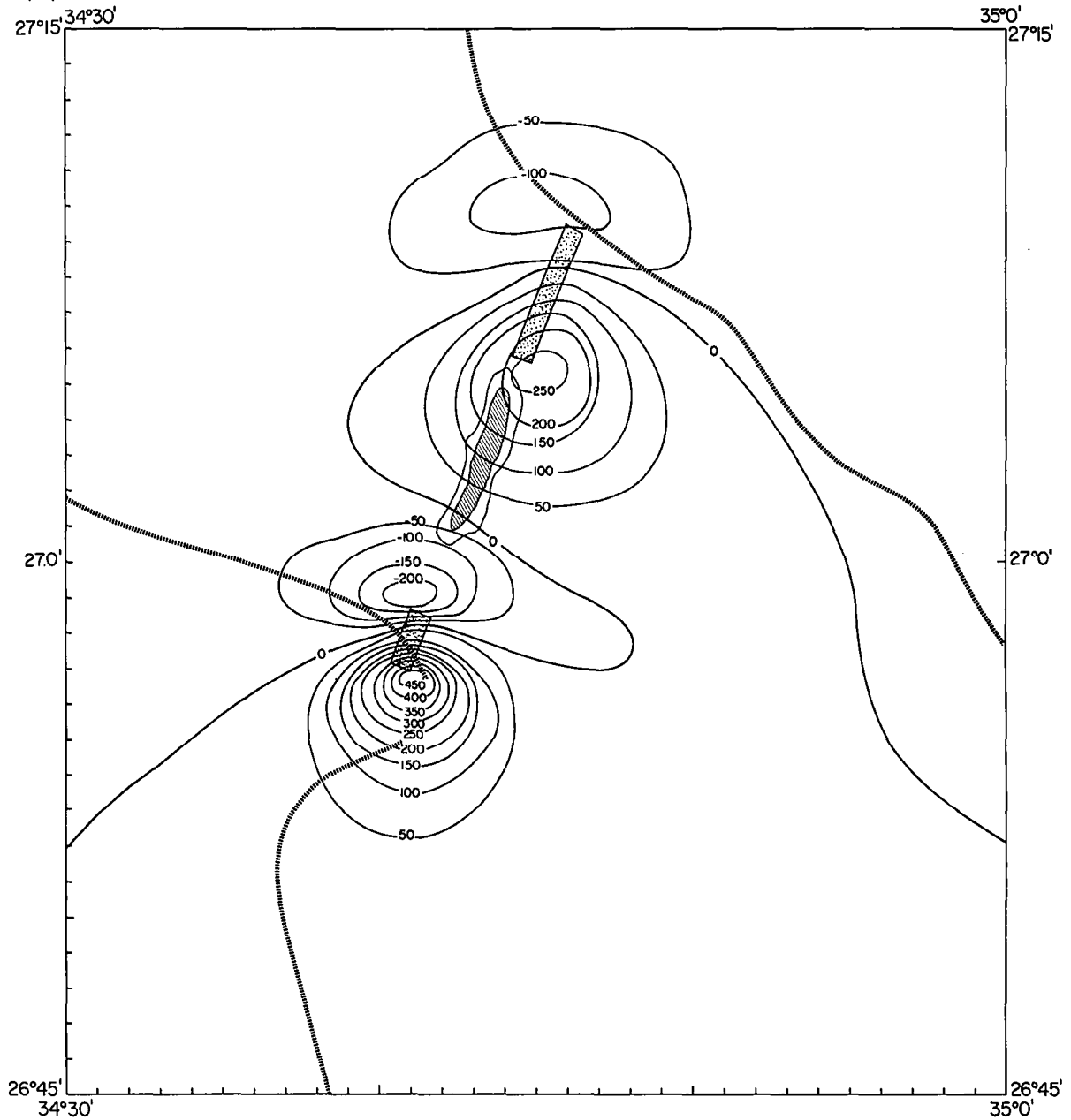


Fig. 8. A. Model total field magnetic anomalies of Conrad Deep region calculated for source bodies oriented perpendicular to the deep. Calculations were made for an equally spaced grid of points at 2 km intervals in the map area shown and contoured at 50 gamma intervals. Source bodies were three-dimensional polygons 1–1.5 km thick with their lower surface 5 km below sea level. A magnetization intensity of 30 A m^{-1} was used with direction given by the geocentric dipole formula. Earth's field direction was that given by IGRF for 1984. Conrad Deep is indicated by the hachured outline and margin scarps are shown as heavy dashed lines. B. Model total magnetic field anomalies of Conrad Deep region calculated for source bodies oriented parallel to the deep. The northern body extends from 5 to 10 km in depth and the southern body extends from 3 to 7 km in depth. Other parameters are as discussed in Fig. 8A.

from the intrusion of the dike can thus be expressed as:

$$T(x, y, z, t) = T_0 \frac{z}{a} + \frac{1}{4} \left[\operatorname{erfc} \frac{(x-x_1)}{\sqrt{4kt}} - \operatorname{erfc} \frac{(x-x_2)}{\sqrt{4kt}} \right] \times \left[\operatorname{erfc} \frac{(y-y_1)}{\sqrt{4kt}} - \operatorname{erfc} \frac{(y-y_2)}{\sqrt{4kt}} \right] \times \left[\sum_{N=1}^{\infty} A_N \operatorname{Sin} \left(\frac{N\pi z}{a} \right) e^{-N^2\pi^2 kt/a^2} \right]$$

where x_1 , x_2 , y_1 and y_2 express the horizontal extent of the dike, k is the thermal diffusivity and the A_N 's are Fourier coefficients of the initial thermal anomaly created by the dike. The last term, in z , expresses the vertical cooling, and the terms in x and y the horizontal cooling of the dike by conduction. Magnetic modeling shows that five to six times the volume of magnetized material is required at each end as in the center to produce a pair of dipolar anomalies. The three-dimensional thermal modeling demonstrates that conductive cooling through the ends of the dike is not sufficient to create such a distribution. A long rectangular dike loses heat most quickly at the top corners and along the top horizontal and vertical edges. The thermal modeling shows that triangular prisms of material cooled below the magnetic blocking temperature form at the same rate along the four top edges of the dike. The cooling at the corners and along the vertical edges does not result in sufficient amounts of additional material cooled below the blocking temperature to form distinct dipole anomalies at each end of the dike. Thus, either massive hydrothermal circulation must be invoked along the faults bounding the axial depression, as is suggested by the low heat flow values at the southwestern fault scarp; or the magnetic anomalies must be assumed to result from two distinct sources. The NW-SE elongation of the magnetic anomalies suggests that these intrusions occurred along the faults. This is also suggested by the deeper and less likely depths (5–10 km) required for the northern source when they are assumed to be parallel to the deep. A small amount of material intruded below the deep, perhaps connecting the two bodies, cannot be ruled out and indeed is suggested by the high heat flow values within the deep. The distribution of

heat flow values does not allow detailed delineation of the geometry of the body as has been done for intrusions in the Gulf of California [18–20].

Whichever model is correct, Conrad Deep is associated with an isolated intrusive event. The high heat flow values indicate that this intrusion occurred relatively recently, since modeling indicates that the conductive heat flow anomaly would be largely dissipated by 40,000 years. The N20°E trend of the deep is the trend of the Gulf of Aqaba and is also commonly found as a fault trend associated with rifting in the Gulf of Suez and on shore around the northern Red Sea [21–24] and has been observed as a prominent lineation by the space shuttle imaging radar [25].

Conrad Deep is located within a well defined axial depression, as is Charcot Deep to the south. The form of the deformation within the axial depression tends to be shorter-wavelength folding and faulting than in the marginal areas where the deformation appears to result from more widely spaced faulting and salt diapirism (Fig. 9). Deformation also extends from depth to the surface more frequently in the axial depression than in the marginal area.

Seismic reflection lines consistently show a thinning of the average post-evaporite sediment thickness towards the axial depression. This could either be the result of tectonic thinning with the greatest extension near the center or of a more abundant sediment supply near the margins. A systematic variation in conductivity with depth in cores collected on the 1984 Conrad cruise [26], which is apparently related to glacial climatic variations, suggests that the sedimentation rates in the center of the Red Sea have been at least as great as those in the marginal areas over the past 100,000 years.

Although the marginal areas show signs of continuing tectonic activity as evidenced by the graben in Fig. 9, these data suggest that the main site of extension and tectonic activity at the present time in the northern Red Sea is the axial depression.

Additional support for this conclusion is provided by the coincidence of the axial depression with the peak of a regional heat flow high that extends completely across the Red Sea rift (Fig. 3) implying that the axial depression marks the location of maximum lithospheric thinning. The coincidence of the axial depression with the maximum

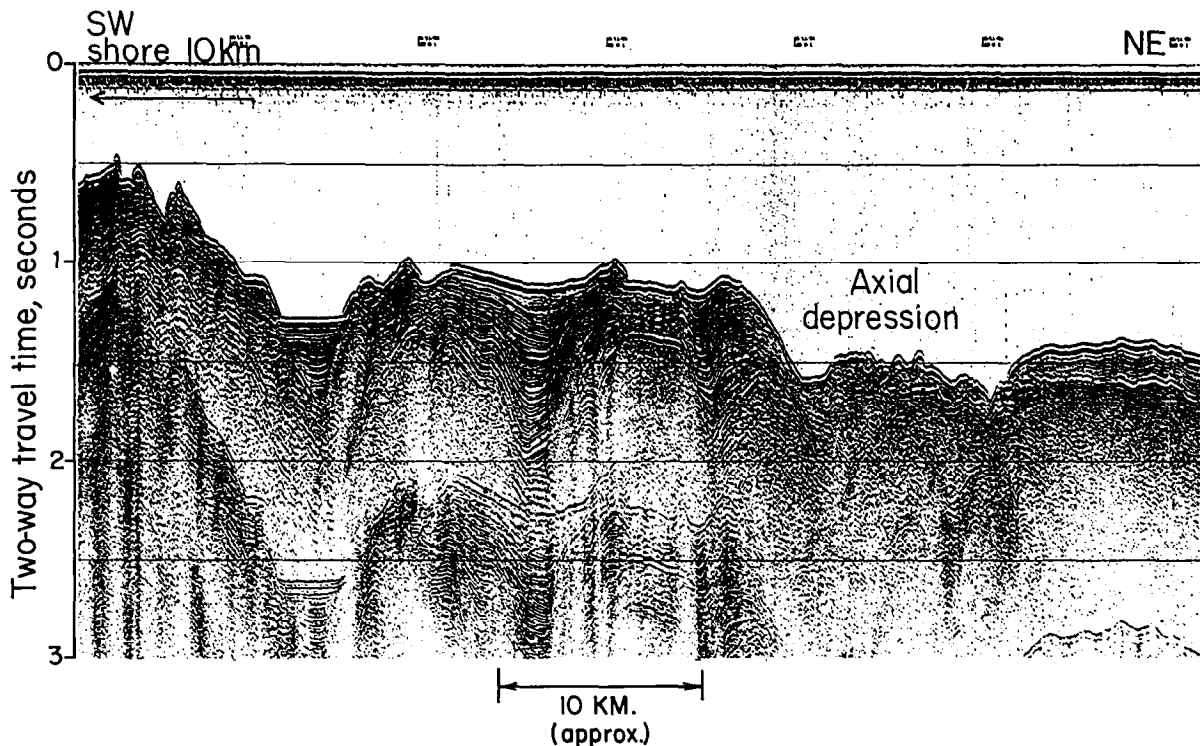


Fig. 9. Water gun seismic reflection line crossing the western margin and axial depression approximately 30 km north of Conrad Deep. The graben 12 km from the southwest end of the profile and the salt diapirs beneath the block between the graben and the axial depression are evidence of continuing deformation on the margins. The shorter-wavelength deformation reaching the surface and the thinner sediments above Reflector S in the axial depression, however, suggests that tectonic activity and extension are now concentrated in the axial depression.

heat flow is further demonstrated by the observation that where the axial depression is offset to the west, the maximum heat flow values are also offset. The interpretation of gravity and seismic data suggests that the marginal areas are made up of a series of rotated fault blocks [27]. The intrusion of isolated bodies into the axial depression at Conrad and Charcot Deeps may mark the first step in the transition from the block faulting type of extension characteristic of the marginal areas to extension largely by intrusion at a localized axis.

5. Summary and conclusions

(1) The newly discovered Conrad Deep is a fairly characteristic "northern" Red Sea deep. It is an elongated, steep sided rift, 10 km long and 2 km wide with a maximum depth of 1460 m. Conrad Deep is located in the center of the Red Sea, 110 km northwest of Charcot Deep and 90 km southeast of the entrance to the Gulf of Suez. It

thus extends the region associated with deeps to the northern end of the Red Sea.

(2) Conrad Deep is associated with large and variable heat flow values ($56\text{--}605\text{ mW m}^{-2}$) and with large amplitude dipolar magnetic anomalies. Detailed modeling shows that the source of the magnetic anomalies are intrusions of highly magnetic bodies into a relatively non-magnetized basement—these intrusions must be roughly 10 km^3 in volume and are located at both ends of the deep, apparently along the faults bounding the axial depression. The high heat flow values within Conrad Deep imply that this intrusion must have occurred relatively recently (within the past 40,000 years).

(3) Both Conrad Deep and Charcot Deep are located within a well defined 10–25 km wide axial depression which marks the axis of deepest water throughout the survey area. The axial depression is located at the peak of a heat flow high extending completely across the Red Sea rift. The presence

of large isolated intrusions within the axial depression may mark the beginning of a transition from the block faulting characteristic of the marginal areas to a more localized axis of extension accompanied by intrusions which may eventually result in the establishment of an organized seafloor spreading axis.

Acknowledgements

We thank Captain J. Peterlin and the officers and crew of R.V. "Robert D. Conrad" for their enthusiastic help during the cruise. We also thank G.A. Dehgheni, and U. ten Brink who helped to gather the shipboard data. This research was supported by N.S.F. grant OCE-83-09983. The manuscript was reviewed by E. Bonatti and M.G. Langseth. Lamont-Doherty Geological Observatory contribution No. 3944.

References

- 1 J.R. Cochran, A model for the development of the Red Sea, *Bull. Am. Assoc. Pet. Geol.* 67, 41–69, 1983.
- 2 H.A. Roeser, A detailed magnetic survey of the southern Red Sea, *Geol. Jahrb.* 13, 131–153, 1975.
- 3 R.C. Searle and D.A. Ross, A geophysical study of the Red Sea axial trough between 20.5° and 22°N, *Geophys. J. R. Astron. Soc.* 43, 555–572, 1975.
- 4 E.T. Degens and D.A. Ross, eds., *Hot Brines and Recent Heavy Metal Deposits in the Red Sea*, 600 pp., Springer-Verlag, New York, N.Y., 1969.
- 5 H. Bäcker and M. Schoell, New deeps with brines and metalliferous sediments in the Red Sea., *Nature Phys. Sci.* 240, 153–158, 1972.
- 6 R.D. Bignell, D.S. Cronan and J.S. Tooms, Red Sea metalliferous brine precipitates, *Geol. Soc. Can. Spec. Paper* 14, 147–179, 1976.
- 7 J. Scheuch, Measurements of heat flow in the Red Sea between 19° and 26° northern latitude (region of the hot brine deeps), *Z. Geophys.* 39, 859–862, 1973.
- 8 E. Bonatti, P. Colantoni, B. Della Vedova and M. Taviani, Geology of the Red Sea transitional zone (22°N–25°N), *Oceanol. Acta* 7, 385–398, 1984.
- 9 E. Bonatti, Punctiform initiation of seafloor spreading in the Red Sea during transition from a continental to an oceanic rift, *Nature* 316, 33–37, 1985.
- 10 S.T. Knott, E.T. Bunce and R.L. Chase, Red Sea seismic reflection studies, in: *The World Rift System*, *Geol. Surv. Can. Spec. Pap.* 66-14, 78–97, 1966.
- 11 J.D. Phillips and D.A. Ross, Continuous seismic reflection profiles in the Red Sea, *Philos. Trans. R. Soc. London, Ser. A*, pp. 143–152, 1970.
- 12 G. Pautot, *Les fosses de la Mer Rouge: approche géomorphologique d'un stade initial d'ouverture océanique réalisée à l'aide du Seabeam*, *Oceanol. Acta* 6, 235–244, 1983.
- 13 G. Pautot, P. Guennoc, A. Coutelle and N. Lyberis, Discovery of a large brine deep in the northern Red Sea, *Nature* 310, 133–136, 1984.
- 14 S.S. Ahmed, Geology and petroleum prospects in eastern Red Sea, *Bull. Am. Assoc. Pet. Geol.* 56, 707–719, 1972.
- 15 J.D. Lowell and G.J. Genik, Seafloor spreading and structural evolution of the southern Red Sea, *Bull. Am. Assoc. Pet. Geol.* 56, 247–259, 1972.
- 16 R.W. Girdler and R.B. Whitmarsh, Miocene evaporites in Red Sea cores, their relevance to the problem of the width and age of oceanic crust beneath the Red Sea, in: R.B. Whitmarsh, O.E. Weser, D.A. Ross et al., *Initial Reports of the Deep Sea Drilling Project*, 23, pp. 913–922, U.S. Government Printing Office, Washington, D.C., 1974.
- 17 M.S. Steckler, The thermal and mechanical evolution of Atlantic-type continental margins, 261 pp., Ph.D. Thesis, Columbia University, New York, N.Y., 1981.
- 18 L.A. Lawver, D.L. Williams and R.P. Von Herzen, A major geothermal anomaly in the Gulf of California, *Nature* 257, 23–28, 1975.
- 19 P. Lonsdale and K. Becker, Hydrothermal plumes, hot springs and conductive heat flow in the Southern Trough of Guaymas Basin, *Earth Planet. Sci. Lett.* 73, 211–225, 1985.
- 20 D.L. Williams, K. Becker, L.A. Lawver and R.P. Von Herzen, Heat flow at the spreading centers of the Guaymas Basin, Gulf of California, *J. Geophys. Res.* 84, 6757–6769, 1979.
- 21 R. Said, *The geology of Egypt*, 377 pp., Elsevier, Amsterdam, 1962.
- 22 D.A. Robson, The structure of the Gulf of Suez (Clysmic) rift, with special reference to the eastern side, *Geol. Soc. London Q. J.* 115, 247–276, 1971.
- 23 D.J. Webster and N. Ritson, Post Eocene stratigraphy of the Suez Rift, *Egyptian General Petroleum Corp., 6th Exploration Seminar*, 20 pp., 1982.
- 24 Z. Garfunkel and Y. Bartov, The tectonics of the Suez rift, *Geol. Surv. Israel Bull.* 71, 44 pp., 1977.
- 25 K. Crane and E. Bonatti, Structural analysis of the Red Sea margins using the space shuttle imaging radar (SIR-A): implications for a propagating rift, *Tectonics*, in press, 1986.
- 26 M.A. Hobart, J.R. Cochran, F. Martinez and M.S. Steckler, The northern Red Sea, III. Heat flow and thermal state of the lithosphere, *EOS* 66, 365, 1985.
- 27 J.R. Cochran, F. Martinez, M.S. Steckler and M.A. Hobart, The northern Red Sea, I. Pre-seafloor spreading tectonics, *EOS* 66, 365, 1985.